

Investigating Brightest Cluster Galaxies: kinematics with SALT

S. I. Loubser

Centre for Space Research, North-West University, Potchefstroom 2520, South Africa

E-mail: Ilani.Loubser@nwu.ac.za

Abstract. We present detailed, high spatial and spectral resolution, longslit observations of four active central cluster galaxies (CCGs) in cooling flow clusters (Abell 0085, 0133, 0644 and Ophiuchus). Our sample consists of CCGs with H α filaments, and have existing data from the X-ray to radio wavelength regimes available. Here, we add the detailed optical data over a broad wavelength range to probe the kinematics of the stars. This, combined with the other multiwavelength data, will form a complete view of the different phases (hot and cold gas and stars) and how they interact in the processes of star formation and feedback detected in central galaxies in cooling flow clusters, as well as the influence of the host cluster.

1. Introduction

The most massive of early-type galaxies – central cluster galaxies (CCGs) – are special. They have extremely high luminosities, diffuse and extended structures, and dominant central locations in clusters. They are believed to be sites of very interesting evolutionary phenomena (e.g. dynamical friction, galactic cannibalism, cooling flows), and may well require there to have been a special process of formation. These processes will leave different imprints in the dynamical properties, the detailed chemical abundances, and the star formation histories of these galaxies, which can be studied using high-quality spectroscopy (Loubser et al. 2008; 2009).

Cooling-flow clusters are common in the local Universe and CCGs are often found at the centres of these systems. If the central cluster density is high enough, and the cooling time of the hot intracluster medium is significantly shorter than the Hubble time (Edge, Stewart & Fabian 1992), intracluster gas could condense and form stars at the bottom of the potential well. The lack of widespread detection of iron lines expected from cluster gas cooling in *XMM-Newton* observations of cool-core clusters contradicted the model that stars are formed in cooling flows (this is sometimes referred to as the “cooling flow problem”). However, previous studies have reported several examples of ongoing star formation in CCGs, in particular those hosted by cooling-flow clusters (Crawford et al. 1999; Loubser et al. 2009).

The central cluster galaxies often host radio-loud AGN, which may account for the necessary heating to counteract radiative cooling (Von der Linden et al. 2007). Thus, CCGs lie at the interface where it is crucial to understand the role of feedback and gas accretion in star formation and also in galaxy and cluster evolution. Within these cooling-flow CCGs, cool molecular clouds, warm ionized hydrogen, and the cooling intracluster medium are related. A complete view of the star formation process necessarily incorporates the stars with the gas and an understanding

Table 1. Galaxies observed with the SALT telescope. All four galaxies show extended H α emission (McDonald et al. 2010). The cluster X-ray temperature (T_X) are from White, Jones & Forman (1997). The values for R_{off} are from Edwards et al. (2007) for ESO541-013 and MCG02-02-086, and for 2MASXJ17122774-2322108 was calculated from information in NED.

Object	Cluster	Redshift z	R_{off} (Mpc)	T_X (keV)	Exposure Time (seconds)
ESO541-013	Abell 0133	0.057	0.017	3.5	9704
MCG-02-02-086	Abell 0085	0.056	0.046	6.5	6353
PGC023233	Abell 0644	0.071	–	6.5	6800
2MASXJ17122774-2322108	Ophiuchus	0.028	0.019	8.6	14030

of the processes by which these phases interact, and therefore, requires information from several wavelength regimes.

We proposed long-slit observations of the stellar populations in active CCGs in cooling-flow clusters. We have selected a sample with confirmed extended H-alpha emission, and with near-infrared (2MASS), ultraviolet (GALEX), X-ray data (Chandra), and in some cases VLA 1.4 GHz fluxes, already available (McDonald et al. 2010).

2. Sample

We have chosen our sample of active central cluster galaxies from the H α imaging presented in McDonald et al. (2010), who in turn, selected their sample from White, Jones & Forman (1997). McDonald et al. (2010) enforced the cuts: $\delta < +35$ deg and $0.025 < z < 0.092$, after which they selected 23 clusters to cover the full range of properties, from very rich clusters with high cooling rates to low-density clusters with small cooling flows. Their classical cooling rates range from $6.3 - 431 M_{\odot} \text{ yr}^{-1}$ which means that while covering a large range in properties, their sample consisted of only cooling flow clusters. From their 23 cooling flow clusters, we selected all the clusters with clearly detected H α in their centres (albeit filamentary, extended or nuclear emission). In addition, all of these central galaxies have optical imaging, near-IR (2MASS) and UV (Galex data) available. Thereafter, we selected all the central galaxies with detailed X-ray (Chandra) data, as well as VLA 1.4 GHz fluxes, available. This resulted in a sub-sample of 10 galaxies. We observed four of these galaxies with the GMOS IFU (as presented in Loubser & Soechting 2013), and we observed four of these galaxies with the SALT RSS. We merely chose the objects with the most auxiliary information available.

3. Observations and data reduction

The data were obtained with the Robert Stobie Spectrograph (RSS) on the SALT telescope between October 2011 and October 2012 (during two observing semesters and on 24 different nights during dark time). The rest wavelength of interest is $4860 - 6731 \text{ \AA}$ (redshifted to $5000 - 7300 \text{ \AA}$). To achieve this, and to avoid losing essential emission lines in the ccd gaps, the pg0900 grating was used with $1.2''$ slit at a carefully selected central wavelength setting. The targets and exposure times are shown in Table 1. In addition to the targets, the necessary flat-fields and arcs frames were also observed at regular intervals, as well as spectrophotometric standard stars for flux calibration. The basic reductions were performed with the PySALT: SALT science pipeline, whilst further reductions were done in IRAF (see Loubser in preparation).

The galaxy and associated error spectra were binned in the spatial direction to ensure a minimum S/N of 30 per \AA in the H β region of the spectrum for measurements as a function of radius. A S/N ratio of 30 per bin was chosen to resolve the optimal number of possible

Table 2. Properties of the CCGs. The PA is given as deg E of N. The half-light radii (r_e) were calculated from the 2MASS catalogue. The last column lists the fraction of the effective half-light radii spanned by the radial profiles measured in this work.

Object	Slit PA (degrees)	Major Axis MA (degrees)	r_e (arcsec)	ϵ	a_e (arcsec)	Fraction times a_e
ESO541-013	197	17	10.63	0.40	10.63	0.87
MCG-02-02-086	149	149	12.10	0.22	12.10	0.71
PGC023233	193	35	6.45	0.14	6.37	0.92
2MASXJ17122774-2322108	135	145	20.06	0.28	19.94	0.16

points, whilst still having acceptable errors on the measurements. Thus, the spatial cross-sections are broader with increasing radius from the centre of the galaxy. In all the profiles plotted here, the values of the measurements are plotted at the luminosity-weighted centres of the spatial bins used to derive the parameters. The effective half-light radius was calculated as $a_e = \frac{r_e(1-\epsilon)}{1-\epsilon |\cos([PA-MA])|}$, with ϵ the ellipticity (data from NED), r_e the radius containing half the light of the galaxy (computed from the 2MASS K -band 20th magnitude arcsec^{-2} isophotal radius as described in Loubser et al. 2008), PA the slit position axis, and MA the major axis.

4. Kinematic measurements

To accurately measure the features of the CCG spectra, we use a combination of the PPF (Cappellari & Emsellem 2004) and GANDALF (Sarzi et al. 2006) routines¹. Gandalf version 1.5 was used as it enables a reddening correction to be performed, and it incorporates errors. This code treats the emission lines as additional Gaussian templates, and solves linearly at each step for their amplitudes and the optimal combination of stellar templates, which are convolved by the best stellar line-of-sight velocity distribution. The stellar continuum and emission lines are fitted simultaneously. All 985 stars of the MILES stellar library (Sánchez-Blázquez et al. 2006) were used as stellar templates to automatically include α -enhancement in the derived optimal template. After the kinematics are fixed, a Gaussian template is constructed for each emission line at each iteration, and the best linear combination of both stellar and emission-line templates (with positive weights) is determined. We have adapted the gandalf code to apply it to the SALT data with a longer wavelength range. None of the four active CCGs contained measureable emission lines despite being surrounded by ionised nebulae in cooling flow clusters. The GANDALF code was used to measure the spatially resolved velocity and velocity dispersion of the absorption spectra. Our slit placement avoided the ionised gas. The spatially resolved velocity and velocity dispersion gradients are shown in Figures 1 and 2. In all the spatially resolved profiles plotted here, the values of the parameters are plotted at the luminosity-weighted centres of the spatial bins used to derive the parameters.

5. Summary

We have exploited SALT to derive the rotational velocity and velocity dispersion profiles for 4 active central cluster galaxies in cooling flow clusters. Despite the undeniably special nature of BCGs due to their extreme morphological properties and locations, the kinematic properties investigated here (rotation and incidence of velocity substructure) seem normal compared with

¹ We make use of the corresponding PPF and GANDALF IDL (Interactive Data Language) codes which can be retrieved at <http://www.leidenuniv.nl/sauron/>.

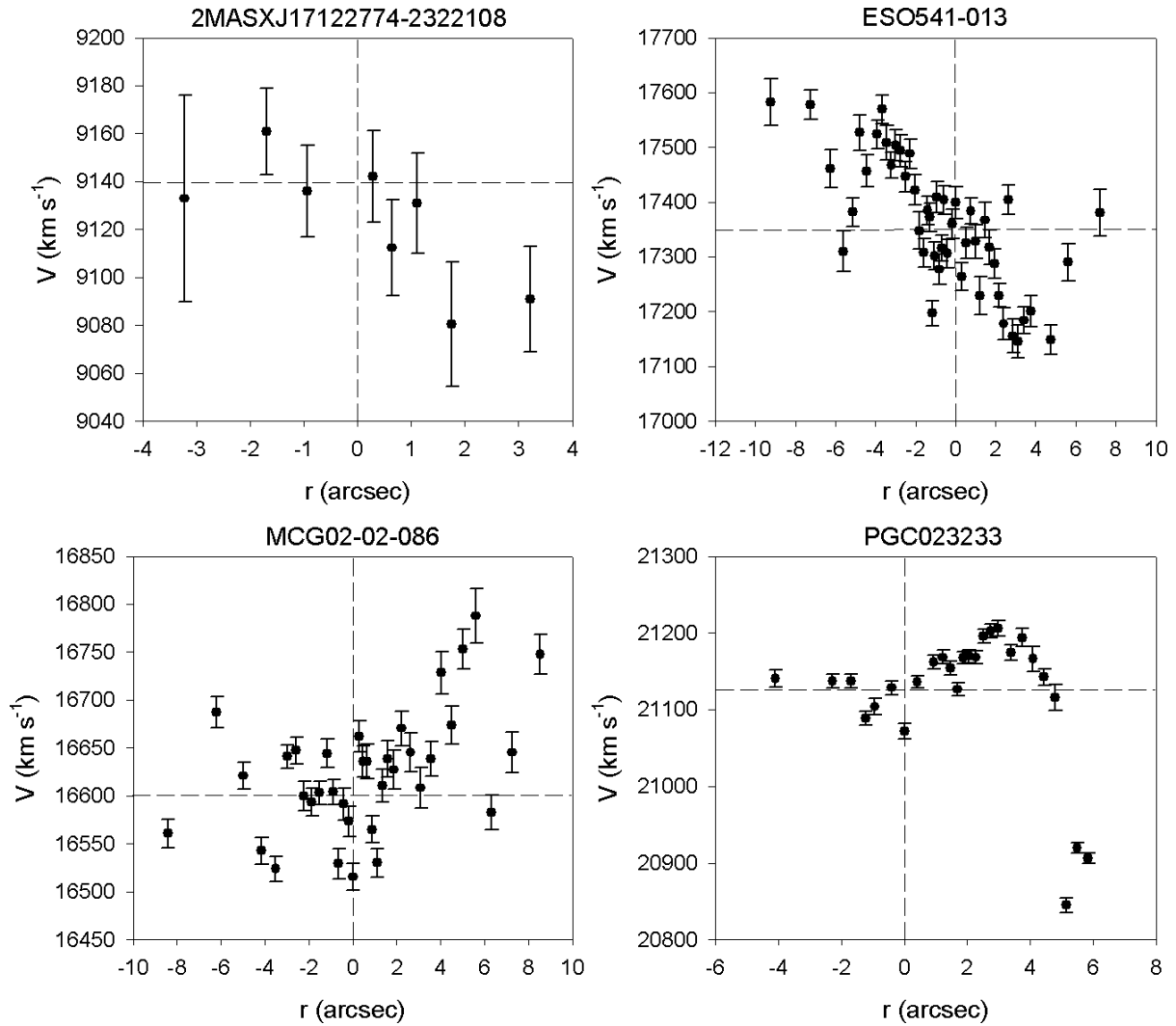


Figure 1. Velocities of the four BCGs. From left to right, top to bottom: 2MASXJ17122774-2322108, ESO541-013, MCG02-02-086, PGC023233.

their ordinary giant elliptical counterparts. Despite the small sample size, we already detect variety in the kinematical properties of these galaxies which is unusual given the homogeneous morphological appearance and similar environments of these galaxies.

We will be adding the detailed stellar population analysis, and place the derived information from the optical spectra in context with multiwavelength data over the full spectrum in a future paper (Loubser, in preparation), to explain the diverse nature of these galaxies.

6. Acknowledgments

SIL is financially supported by the South African National Research Foundation.

7. References

- [1] Cappellari M and Emsellem E 2004 *PASP*. **116** 138
- [2] Crawford C S, Allen S W, Ebeling H, Edge A C, Fabian A C 1999 *MNRAS*. **306** 857
- [3] Edge A C, Stewart G C, Fabian A C 1992 *MNRAS*. **258** 177
- [4] Edwards L O V, Hudson M J, Balogh M L, Smith R J 2007 *MNRAS*. **379** 100

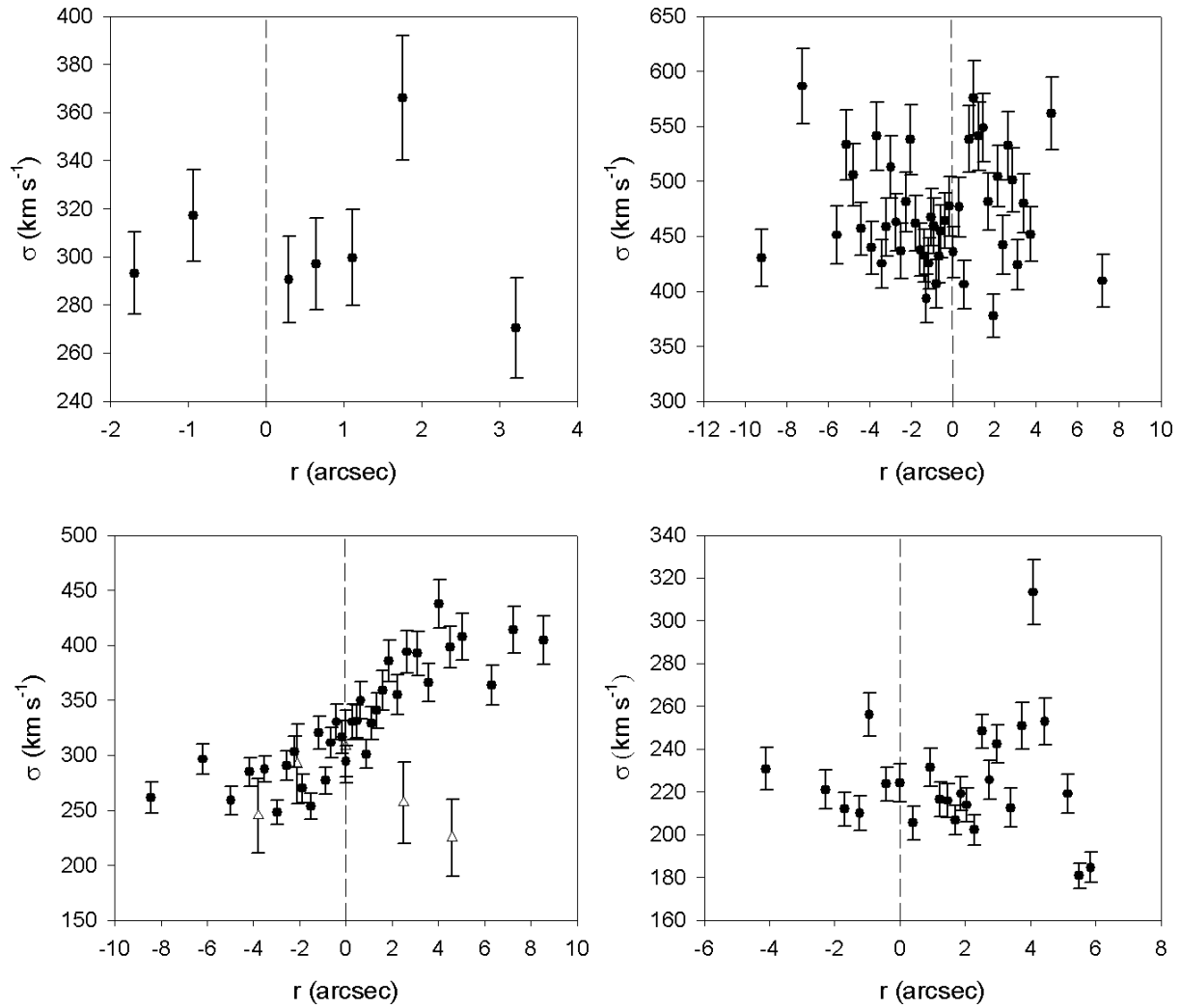


Figure 2. Velocity dispersion of the four BCGs. From left to right, top to bottom: 2MASXJ17122774-2322108, ESO541-013, MCG02-02-086, PGC023233. The empty triangles in MCG02-02-086 is data from Fisher et al. (1995) also taken along the major axis and shown here as comparison.

- [5] Fisher D, Illingworth G, Franx M 1995 *ApJ*. **438** 539
- [6] Loubser S I, Sansom A E, Sánchez-Blázquez P, Soechting I K, Bromage G 2008 *MNRAS*. **391** 1009
- [7] Loubser S I, Sánchez-Blázquez P, Sansom A E, Soechting I K 2009 *MNRAS*. **398** 133
- [8] Loubser S I and Soechting I K 2013 *MNRAS*. **431** 2933
- [9] McDonald M, Veilleux S, Rupke D S N, Mushotzky R 2010 *ApJ*. **721** 1262
- [10] Sánchez-Blázquez P et al. 2006 *MNRAS* **371** 703
- [11] Sarzi M et al. 2006 *MNRAS*. **366** 1151
- [12] Von der Linden A, Best P N, Kauffmann G, White S D M 2007 *MNRAS*. **379** 867
- [13] White D A, Jones C, Forman W 1997 *MNRAS* **292** 419